Intensity correlations, entanglement properties, and ghost imaging in multimode thermal-seeded parametric down-conversion: Theory

Ivo P. Degiovanni,[1] Maria Bondani,[2] Emiliano Puddu,[3,4] Alessandra Andreoni,[3,4] and Matteo G. A. Paris[5,6]
[1]*Istituto Nazionale di Ricerca Metrologica, Torino, Italy*
[2]*National Laboratory for Ultrafast and Ultraintense Optical Science—C.N.R.-I.N.F.M., Como, Italy*
[3]*Dipartimento di Fisica e Matematica, Università degli Studi dell'Insubria, Como, Italy*
[4]*Consiglio Nazionale delle Ricerche, Istituto Nazionale per la Fisica della Materia (C.N.R.-I.N.F.M.), Como, Italy*
[5]*Dipartimento di Fisica e Matematica, Università degli Studi dell'Insubria, Como, Italy*
[6]*I.S.I. Foundation, I-10133 Torino, Italy*
(Received 12 July 2007; published 14 December 2007)

We address parametric down-conversion seeded by multimode pseudothermal fields. We show that this process may be used to generate multimode pairwise correlated states with entanglement properties that can be tuned by controlling the seed intensities. Parametric down-conversion seeded by multimode pseudothermal fields represents a source of correlated states, which allows one to explore the classical-quantum transition in pairwise correlations and to realize ghost imaging and ghost diffraction in regimes not yet explored by experiments.

DOI: 10.1103/PhysRevA.76.062309 PACS number(s): 03.67.Mn, 42.50.Dv, 42.65.Lm

I. INTRODUCTION

Ghost imaging [1] and ghost diffraction [2] consist of the retrieval of an object transmittance pattern or its Fourier transform, respectively, by evaluating a fourth-order correlation function at the detection planes between the field that never interacted with the object and a correlated one transmitted by the object. A general ghost-imaging–ghost-diffraction scheme involves a source of correlated bipartite fields and two propagation arms usually called test (T) and reference (R). In the T arm, where the object is placed, a bucket (or a pointlike) detector measures the total light transmitted by it. The R arm contains an optical setup suitable for reconstructing the image of the object or its Fourier transform and a position-sensitive detector [3].

The correlations needed for ghost imaging and ghost diffraction may be either quantum, as those shown by entangled states produced by spontaneous parametric down-conversion (PDC) [1] or classical, as those present in the fields at the output of a beam-splitter fed with a multimode pseudothermal beam [4–6]. In recent years several authors discussed analogies and differences between the two cases in terms of the achievable visibility and of the optical configurations needed for image reconstruction. A history of this debate from different points of view may be found in Ref. [3] and references therein. Recently, it has been suggested that the entangled nature of the light source [7–9] may be necessary to satisfy the "back-propagating" thin-lens equation, which, indeed, is fulfilled by PDC-based ghost-imaging systems. Among other things, we prove that this claim is incorrect.

In this paper, we discuss the use of a PDC-based light source for ghost imaging and diffraction. In our scheme (see Fig. 1), the nonlinear crystal realizing PDC is seeded by two multimode thermal (MMT) beams. We show that the entanglement properties and the amount of correlation at the output may be tuned by changing the intensities of the seeds, thus leading to a source that can be used to investigate the transition from the classical to the quantum regime. Besides, our source allows ghost-image reconstruction with the same optical scheme used for ghost imaging based on spontaneous PDC, with the "back-propagating" thin-lens equation that is satisfied irrespective of the entanglement of the state. We notice that the effectiveness of the setup discussed here has already been demonstrated in the case of a crystal seeded with a single MMT beam [10].

The paper is structured as follows. In Sec. II we calculate the state obtained from our PDC source with the injection of MMT seeds on both the T and R arms, thus revealing that the output field on each arm maintains the statistics of the seed. In Sec. III we analyze both the intensity correlations between the output beams and the entanglement properties of the overall state. We explicitly evaluate separability thresholds in terms of the seed intensities, and show that the condition for the existence of nonclassical correlations in intensity measurements subsumes the condition for inseparability, i.e., sub-shot-noise correlations are a sufficient condition for entanglement in our system. We also show that entanglement properties of the output field are not affected by losses taking place after the PDC interaction. In Sec. IV we show that the state generated in our scheme satisfies the "back-propagating" thin-lens equation independently on the seed intensities, i.e., independently of being entangled or not, and it is suitable for realizing ghost-imaging and ghost-diffraction experiments. Finally, Sec. V closes the paper with some concluding remarks.

II. PARAMETRIC DOWN-CONVERSION WITH THERMAL SEEDS

The interaction scheme we are going to consider is sketched in Fig. 1. It consists of a nonlinear $\chi^{(2)}$ crystal pumped by a monochromatic nondepleted plane wave propagating along the z axis. The Hamiltonian describing the resulting parametric process is given by

$$H_I = \int d^2\mathbf{r} \int_0^L dz\, \chi^{(2)} E_p(\mathbf{x},t) a_T(\mathbf{x},t) a_R(\mathbf{x},t) + \text{H.c.}, \quad (1)$$

L being the crystal length and $\chi^{(2)}$ the nonlinear susceptibility. The pump field may be written as $E_p(\mathbf{x},t) = \mathcal{E}_p \exp[i(\Omega_p t - K_p z)]$ [11].

We can write the interacting quantum fields as

$$a_j(\mathbf{x},t) \propto \sum_{\mathbf{q}_j,\nu_j} a_{j,\mathbf{q}_j,\nu_j} e^{i[K_{j,z}z + \mathbf{q}_j\cdot\mathbf{r} - (\Omega_j+\nu_j)t]} \quad (j = R,T), \quad (2)$$

where $\mathbf{q}_j$ is the transverse momentum and $K_{j,z}$ is the magnitude of the longitudinal momentum, $K_{j,z} = \sqrt{K_j^2 - q_j^2}$, being $K_j = n_j(\Omega_j + \nu_j)/c$, with n_j the index of refraction, Ω_j the selected central frequency in channel j, ν_j the frequency displacement with respect to Ω_j, and c the speed of light in the vacuum. The commutation relation of the quantum fields are

$$[a_{j,\mathbf{q},\nu}, a^\dagger_{j',\mathbf{q}',\nu'}] = \delta_{j,j'}\delta_{\mathbf{q},\mathbf{q}'}\delta_{\nu,\nu'} \quad (j,j' = R,T),$$

$$[a_{j,\mathbf{q},\nu}, a_{j',\mathbf{q}',\nu'}] = 0. \quad (3)$$

The evolution of a quantum system induced by the interaction Hamiltonian in Eq. (1) is described by the unitary operator $U = \exp(-i\hbar^{-1}\int H_I dt)$, where

$$-\frac{i}{\hbar}\int H_I dt = i\sum_{\mathbf{q},\nu} \kappa_{\mathbf{q},\nu} a_{T,\mathbf{q},\nu} a_{R,-\mathbf{q},-\nu} + \text{H.c.}, \quad (4)$$

where $\kappa_{\mathbf{q},\nu} \propto \text{sinc}[(K_p - K_{T,z} - K_{R,z})L/2]$. To obtain Eq. (4) we have exploited the conservation of energy at the central wavelength $\Omega_p = \Omega_T + \Omega_R$ obtaining $\nu_T = -\nu_R = \nu$, and the conservation of transverse momentum $\mathbf{q}_T = -\mathbf{q}_R = \mathbf{q}$. As, according to Eq. (4), the extension to the nonmonochromatic case is, in most cases, straightforward, in the following analysis we will focus on the monochromatic emission at the frequencies Ω_R and Ω_T and hence we will drop the subscript ν from the variables.

The operator U can be rewritten in terms of the operators $S_\mathbf{q} = (\kappa_\mathbf{q} a_{T,\mathbf{q}} a_{R,-\mathbf{q}} + \text{H.c.})$ as $U = \exp(i\Sigma_\mathbf{q} S_\mathbf{q})$. According to the commutation relations in Eq. (3), we have $[S_\mathbf{q}, S_{\mathbf{q}'}] = 0$, and therefore $U = \otimes_\mathbf{q} e^{iS_\mathbf{q}}$, i.e., the interaction establishes pairwise correlations among the modes.

In our analysis we focus on the case in which both the T and R arms are seeded with uncorrelated MMT beams

$$\rho_{\text{in}} = \bigotimes_\mathbf{q} \rho_{T,\mathbf{q}} \otimes \rho_{R,-\mathbf{q}},$$

$$\rho_{j,\mathbf{q}} = \sum_{n=0}^{\infty} P_{j,\mathbf{q}}(n) |n\rangle_{j,\mathbf{q}j,\mathbf{q}} \langle n|, \quad (5)$$

where $j = R,T$ and $|n\rangle_{j,\mathbf{q}}$ denotes the Fock number basis for the mode $\mathbf{q}$ of the j arm. The thermal probability distribution of the input is given by

$$P_{j,\mathbf{q}}(n) = \mu_{j,\mathbf{q}}^n (1 + \mu_{j,\mathbf{q}})^{-n-1},$$

$\mu_{j,\mathbf{q}}$ being the average photon number per mode. The density matrix at the output is given by

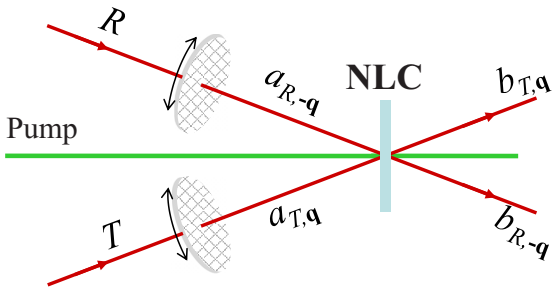

FIG. 1. (Color online) Schematic diagram of the nonlinear interaction. T and R are the test and reference arms of the setup.

$$\rho_{\text{out}} = U\rho_{\text{in}}U^\dagger = \bigotimes_\mathbf{q} e^{iS_\mathbf{q}} \rho_{T,\mathbf{q}} \otimes \rho_{R,-\mathbf{q}} e^{-iS_\mathbf{q}}. \quad (6)$$

According to [12], it is possible to "disentangle" $e^{iS_\mathbf{q}}$ by using the two-boson representation of the SU(1,1) algebra as

$$e^{iS_\mathbf{q}} = \exp\{\zeta_\mathbf{q} a^\dagger_{T,\mathbf{q}} a^\dagger_{R,-\mathbf{q}}\} \exp\{-\eta_\mathbf{q}(a^\dagger_{T,\mathbf{q}} a_{T,\mathbf{q}} + a^\dagger_{R,-\mathbf{q}} a_{R,-\mathbf{q}} + 1)\} \times \exp\{-\zeta^*_\mathbf{q} a_{T,\mathbf{q}} a_{R,-\mathbf{q}}\}, \quad (7)$$

where $\zeta_\mathbf{q} = -ie^{-i\varphi_\mathbf{q}} \tanh(|\kappa_\mathbf{q}|)$, $\eta_\mathbf{q} = \ln[\cosh|\kappa_\mathbf{q}|]$, and $e^{i\varphi_\mathbf{q}} = \kappa_\mathbf{q}/|\kappa_\mathbf{q}|$.

Equation (7) implies that

$$e^{iS_\mathbf{q}} |n\rangle_{T,\mathbf{q}} \otimes |m\rangle_{R,-\mathbf{q}} = \sum_{k=0}^{\min\{m,n\}} \sum_{l=0}^{\infty} C_\mathbf{q}(m,n,k,l) |n-k+l\rangle_{T,\mathbf{q}} \otimes |m-k+l\rangle_{R,-\mathbf{q}}, \quad (8)$$

with

$$C_\mathbf{q}(m,n,k,l) = e^{-\eta_\mathbf{q}(n+m-2k+1)} \times \frac{\sqrt{n!\,m!\,(n-k+l)!\,(m-k+l)!}}{k!\,l!\,(n-k)!\,(m-k)!} \zeta_\mathbf{q}^l (-\zeta^*_\mathbf{q})^k. \quad (9)$$

By substituting Eq. (8) in Eq. (6) we obtain the output state in the Schrödinger picture as

$$\rho_{\text{out}} = \bigotimes_\mathbf{q} \sum_{nm} P_{T,\mathbf{q}}(n) P_{R,-\mathbf{q}}(m) \sum_{k_1,k_2=0}^{\min\{m,n\}} \sum_{l_1,l_2=0}^{\infty} C_\mathbf{q}(m,n,k_1,l_1) \times C_\mathbf{q}(m,n,k_2,l_2)^* |n-k_1+l_1\rangle_{T,\mathbf{q}T,\mathbf{q}} \langle n-k_2+l_2| \otimes |m-k_1+l_1\rangle_{R,-\mathbf{q}R,-\mathbf{q}} \langle m-k_2+l_2|. \quad (10)$$

Meanwhile, in the Heisenberg description, the modes after the interaction with the crystal are given by $b_{j,\mathbf{q}} = U^\dagger a_{j,\mathbf{q}} U$, i.e.,

$$b_{j,\mathbf{q}} = \mathcal{U}_\mathbf{q} a_{j,\mathbf{q}} + e^{i\varphi_\mathbf{q}} \mathcal{V}_\mathbf{q} a^\dagger_{j',-\mathbf{q}} \quad (j,j' = R,T,\ j \neq j'), \quad (11)$$

where $\mathcal{U}_\mathbf{q} = \cosh|\kappa_\mathbf{q}|$ and $\mathcal{V}_\mathbf{q} = \sinh|\kappa_\mathbf{q}|$ (and obviously $\mathcal{U}_\mathbf{q} = \mathcal{U}_{-\mathbf{q}}$, $\mathcal{V}_\mathbf{q} = \mathcal{V}_{-\mathbf{q}}$, and $\varphi_\mathbf{q} = \varphi_{-\mathbf{q}}$). Equation (11) represents the quantum dynamical evolution of the system i.e., the input-output relations of the parametric process. Of course, they are independent on the initial states and are valid in any working regime, i.e., for any input state and for any value of the pump intensity within the parametric approximation. This

includes the two-photon regime as well as the continuous variable regime. On the other hand, the entanglement properties of the output state strongly depend on the initial state. In the following section we discuss in detail the entanglement properties for the case of thermal light at the input.

As expected, the first moments of the photon distribution for each mode are those of a thermal statistics

$$\langle n_{T,\mathbf{q}}\rangle = \mu_{T,\mathbf{q}} + n_{\mathrm{PDC},\mathbf{q}}(1+\mu_{T,\mathbf{q}}+\mu_{R,-\mathbf{q}}),$$

$$\langle n_{R,-\mathbf{q}}\rangle = \mu_{R,-\mathbf{q}} + n_{\mathrm{PDC},\mathbf{q}}(1+\mu_{T,\mathbf{q}}+\mu_{R,-\mathbf{q}}),$$

$$\langle (\Delta n_{T,\mathbf{q}})^2\rangle = \langle n_{T,\mathbf{q}}\rangle(\langle n_{T,\mathbf{q}}\rangle+1),$$

$$\langle (\Delta n_{R,-q})^2\rangle = \langle n_{R,-\mathbf{q}}\rangle(\langle n_{R,-\mathbf{q}}\rangle+1), \tag{12}$$

where $\langle O\rangle = \mathrm{Tr}[O\rho_{\mathrm{out}}] = \mathrm{Tr}[U^\dagger O U \rho_{\mathrm{in}}]$ (Schrödinger and Heisenberg picture, respectively), $\Delta O = O - \langle O\rangle$, and $n_{\mathrm{PDC},\mathbf{q}} = \sinh^2|\kappa_{\mathbf{q}}|$ is the average number of photons due to spontaneous PDC.

Notice that the case of vacuum inputs, $\rho_{\mathrm{in}} = |0\rangle\langle 0|_T \otimes |0\rangle\langle 0|_R$, corresponds to spontaneous down-conversion, i.e., to the generation of twin-beam, whereas the case of a single MMT on one arm and the vacuum on the other, $\rho_{\mathrm{in}} = \otimes_{\mathbf{q}}(|0\rangle\langle 0|_{T,\mathbf{q}} \otimes \rho_{R,-\mathbf{q}})$, corresponds to the state considered in Ref. [10].

III. ENTANGLEMENT AND INTENSITY CORRELATIONS

In this section we address intensity correlations and entanglement properties of the beams generated in our scheme. As we will see, the amount of nonclassical correlations and entanglement can be tuned upon changing the intensity of the thermal seeds and there exist thresholds for the appearance of those nonclassical features. On the other hand, the index of total correlations (either classical or quantum) is a monotonically increasing function of both the seed and the PDC energy.

A. Entanglement and separability

The down-conversion process is known to provide pairwise entanglement between signal and idler beams. In our notations the (possibly) entangled modes are $a_{T,\mathbf{q}}$ and $a_{R,-\mathbf{q}}$. In the spontaneous process the output state is entangled for any value of the parametric gain (i.e., for any value of the crystal susceptibility, length, etc.), whereas in the case of a thermally seeded crystal the degree of entanglement crucially depends on the intensity of the seeds.

Since thermal states are Gaussian and the PDC Hamiltonian is bilinear in the field modes, the overall output state is also Gaussian. Therefore, the entanglement properties may be evaluated by checking the positivity of the partial transpose (PPT condition), which represents a sufficient and necessary condition for separability for Gaussian pairwise mode entanglement [13]. Gaussian states are completely characterized by their covariance matrix. In this context let us introduce the "position"(-like) operators X and "momentum" (-like) operators Y

$$X_{j,\mathbf{q}} = \frac{a_{j,\mathbf{q}} + a_{j,\mathbf{q}}^\dagger}{\sqrt{2}},$$

$$Y_{j,\mathbf{q}} = \frac{a_{j,\mathbf{q}} - a_{j,\mathbf{q}}^\dagger}{i\sqrt{2}} \quad (j=R,T). \tag{13}$$

Introducing the vector operator

$$\xi = (X_{T,\mathbf{q}_1}, Y_{T,\mathbf{q}_1}, X_{R,-\mathbf{q}_1}, Y_{R,-\mathbf{q}_1}, \ldots)^T, \tag{14}$$

with $m=1,2,\ldots,\infty$, from the commutation relations in Eq. (3) gives

$$[\xi_\alpha, \xi_\beta] = i\Omega_{\alpha,\beta}, \tag{15}$$

where $\mathbf{\Omega} = \oplus_m \omega \oplus \omega$ and ω is the symplectic matrix

$$\omega = \begin{pmatrix} 0 & 1 \\ -1 & 0 \end{pmatrix}. \tag{16}$$

The covariance matrix V is calculated as $V_{\alpha,\beta} = 2^{-1}\langle\{\Delta\xi_\alpha, \Delta\xi_\beta\}\rangle$, where $\{O_1, O_2\}$ denotes the anticommutator. Uncertainty relation among the position and momentum operators impose a constraint on the covariance matrix, $\mathbf{V} + \frac{i}{2}\mathbf{\Omega} \geq 0$, corresponding to the positivity of the state. The input-output relations for position and momentum operators are calculated according to Eq. (11), obtaining

$$U^\dagger X_{j,\mathbf{q}} U = \mathcal{U}_{\mathbf{q}} X_{j,\mathbf{q}} + \mathcal{V}_{\mathbf{q}} X_{j',-\mathbf{q}},$$

$$U^\dagger Y_{j,\mathbf{q}} U = \mathcal{U}_{\mathbf{q}} Y_{j,\mathbf{q}} - \mathcal{V}_{\mathbf{q}} Y_{j',-\mathbf{q}} \quad (j,j'=R,T,\ j\neq j'). \tag{17}$$

Without any loss of generality, in the derivation of Eqs. (17) we set $\varphi_{\mathbf{q}}=0$, which, in turn, corresponds to a proper choice of the phase or, equivalently, to a proper redefinition of the operators $a_{j,\mathbf{q}}$ that amounts to a rotation of the phase space. From Eqs. (17) we calculate the covariance matrix

$$\mathbf{V} = \bigoplus_{m=1}^{\infty} \mathbf{V}_{\mathbf{q}_m} = \begin{pmatrix} \mathbf{V}_{\mathbf{q}_1} & 0 & 0 & \cdots \\ 0 & \mathbf{V}_{\mathbf{q}_2} & 0 & \cdots \\ 0 & 0 & \mathbf{V}_{\mathbf{q}_3} & \cdots \\ \vdots & \vdots & \vdots & \ddots \end{pmatrix} \tag{18}$$

with

$$\mathbf{V}_{\mathbf{q}} = \begin{pmatrix} \mathcal{A}_{\mathbf{q}} & 0 & \mathcal{C}_{\mathbf{q}} & 0 \\ 0 & \mathcal{A}_{\mathbf{q}} & 0 & -\mathcal{C}_{\mathbf{q}} \\ \mathcal{C}_{\mathbf{q}} & 0 & \mathcal{B}_{\mathbf{q}} & 0 \\ 0 & -\mathcal{C}_{\mathbf{q}} & 0 & \mathcal{B}_{\mathbf{q}} \end{pmatrix}, \tag{19}$$

where

$$\mathcal{A}_{\mathbf{q}} = [\mathcal{U}_{\mathbf{q}}^2(2\mu_{T,\mathbf{q}}+1) + \mathcal{V}_{\mathbf{q}}^2(2\mu_{R,-\mathbf{q}}+1)]/2,$$

$$\mathcal{B}_{\mathbf{q}} = [\mathcal{U}_{\mathbf{q}}^2(2\mu_{R,-\mathbf{q}}+1) + \mathcal{V}_{\mathbf{q}}^2(2\mu_{T,\mathbf{q}}+1)]/2,$$

$$\mathcal{C}_{\mathbf{q}} = \mathcal{U}_{\mathbf{q}}\mathcal{V}_{\mathbf{q}}(\mu_{T,\mathbf{q}} + \mu_{R,-\mathbf{q}} + 1). \tag{20}$$

$\mathbf{V}$ satisfies the uncertainty relations ensuring the positivity of ρ_{out}.

In order to check whether and when the state ρ_{out} is entangled we apply the PPT criteria for Gaussian entanglement [13]. For instance, we apply the positive map $\mathcal{L}_{R,-\mathbf{q}'}$ to the state ρ_{out}. $\mathcal{L}_{R,-\mathbf{q}'}(\rho_{\text{out}})$ is the transposition (complex conjugation) only of the subspace $\mathcal{H}_{R,-\mathbf{q}'}$ corresponding to the mode $R,-\mathbf{q}'$. Simon showed that this corresponds to calculation of the covariance matrix $\tilde{\mathbf{V}}$, where all the matrix blocks $\mathbf{V}_{\mathbf{q}}$ remain the same except for the matrix $\mathbf{V}_{\mathbf{q}'} \rightarrow \tilde{\mathbf{V}}_{\mathbf{q}'}$. $\tilde{\mathbf{V}}_{\mathbf{q}'}$ is calculated with a sign change in the $R,-\mathbf{q}'$ momentum variable ($Y_{R,-\mathbf{q}'} \rightarrow -Y_{R,-\mathbf{q}'}$), while the other momentum and position variables remain unchanged ($X_{T,\mathbf{q}'} \rightarrow X_{T,\mathbf{q}'}$, $Y_{T,\mathbf{q}'} \rightarrow Y_{T,\mathbf{q}'}$, and $X_{R,-\mathbf{q}'} \rightarrow X_{R,-\mathbf{q}'}$). Thus we obtain

$$\tilde{\mathbf{V}}_{\mathbf{q}'} = \begin{pmatrix} \mathcal{A}_{\mathbf{q}'} & 0 & \mathcal{C}_{\mathbf{q}'} & 0 \\ 0 & \mathcal{A}_{\mathbf{q}'} & 0 & \mathcal{C}_{\mathbf{q}'} \\ \mathcal{C}_{\mathbf{q}'} & 0 & \mathcal{B}_{\mathbf{q}'} & 0 \\ 0 & \mathcal{C}_{\mathbf{q}'} & 0 & \mathcal{B}_{\mathbf{q}'} \end{pmatrix}, \tag{21}$$

where $\mathcal{A}_{\mathbf{q}'}$, $\mathcal{B}_{\mathbf{q}'}$, and $\mathcal{C}_{\mathbf{q}'}$ are defined in Eqs. (20). According to PPT criteria, the separability of ρ_{out} is guaranteed by the positivity of $\mathcal{L}_{R,-q'}(\rho_{\text{out}})$, i.e.,

$$\tilde{\mathbf{V}} + \frac{i}{2}\mathbf{\Omega} \geq 0. \tag{22}$$

Inequality in Eq. (22) corresponds to

$$\mu_{T,\mathbf{q}'}\mu_{R,-\mathbf{q}'} - n_{\text{PDC},\mathbf{q}'}(1 + \mu_{T,\mathbf{q}'} + \mu_{R,-\mathbf{q}'}) \geq 0. \tag{23}$$

We observe that the spontaneous PDC corresponds to the situation with $\mu_{T,\mathbf{q}'} = \mu_{R,-\mathbf{q}'} = 0$; thus ρ_{out} is entangled. Also the case considered in Ref. [10], a MMT seeded PDC only on one arm (i.e., $\mu_{R,-\mathbf{q}'} = 0$), is always entangled. On the contrary, in the case of MMT seeded PDC on both arms, inequality in Eq. (23) introduces a threshold. For instance, if we consider a MMT seed with the same mean number of photon per mode, μ, only when the inequality $\mu^2 \geq n_{\text{PDC},\mathbf{q}}(1+2\mu)$ is satisfied, ρ_{out} is separable. It is noteworthy to observe that if the PPT is applied to any other subspaces the inequalities obtained are analogous to Eq. (23), and thus the result is the same.

B. Separability and losses

Here we address the problem of the effect of the losses on the separability of the state in Eq. (10). In fact the presence of losses, e.g., internal reflection or absorption in the nonlinear crystal, may modify the quantum properties of the state, in particular the transition from entanglement to separability, which, in the absence of losses, is marked by the condition in Eq. (23).

Losses in a quantum channel can be modeled by a beam splitter, in one port of which the quantum channel is injected while the vacuum enters the other port. The model implies that Gaussian states after interaction are still Gaussian states due to the bilinearity of the beam-splitter Hamiltonian. Thus, also in the presence of losses, the covariance matrix completely describes the quantum state. If we consider an overall transmission factor τ on both channels we obtain the covariance matrix $\mathbf{V}_\tau = \tau\mathbf{V} + (1-\tau)1/2$. The form of the covariance matrix $\mathbf{V}_\tau$ is completely analogous to Eq. (18), where the block matrices $\mathbf{V}_{\mathbf{q}}$ are substituted with the block matrices $\mathbf{V}_{\tau,\mathbf{q}}$. $\mathbf{V}_{\tau,\mathbf{q}}$ has the same structure of $\mathbf{V}_{\mathbf{q}}$ in Eq. (19), where $\mathcal{A}_{\mathbf{q}}$, $\mathcal{B}_{\mathbf{q}}$, and $\mathcal{C}_{\mathbf{q}}$ are substituted by

$$\mathcal{A}_{\tau,\mathbf{q}} = \{1 + 2\tau[\mathcal{U}_{\mathbf{q}}^2\mu_{T,\mathbf{q}} + \mathcal{V}_{\mathbf{q}}^2(\mu_{R,-\mathbf{q}} + 1)]\}/2,$$

$$\mathcal{B}_{\tau,\mathbf{q}} = \{1 + 2\tau[\mathcal{U}_{\mathbf{q}}^2\mu_{R,-\mathbf{q}} + \mathcal{V}_{\mathbf{q}}^2(\mu_{T,\mathbf{q}} + 1)]\}/2,$$

and

$$\mathcal{C}_{\tau,\mathbf{q}} = \tau\mathcal{C}_{\mathbf{q}},$$

respectively. Thus, following the same line of thought of Sec. III A we obtain the covariance matrix $\tilde{\mathbf{V}}_\tau$, corresponding to the partial transposition of the state. According to PPT separability criteria, the state is separable if and only if the inequality $\tilde{\mathbf{V}}_\tau + \frac{i}{2}\mathbf{\Omega} \geq 0$ is fulfilled. This condition can be rewritten as

$$\tau^2[\mu_{T,\mathbf{q}'}\mu_{R,-\mathbf{q}'} - n_{\text{PDC},\mathbf{q}'}(1 + \mu_{T,\mathbf{q}'} + \mu_{R,-\mathbf{q}'})] \geq 0. \tag{24}$$

Since Eq. (24) is fully equivalent to Eq. (23), we conclude that losses do not affect the entanglement properties of the state in Eq. (10).

C. Intensity correlations

We now evaluate the pairwise intensity correlations possessed by the generated beams. In addition, we analyze the connections between threshold for separability and the threshold required to have nonclassical correlations. As we will see a state obtained by thermally seeded PDC that exhibits sub-shot-noise correlations is entangled, whereas the converse is not necessarily true. In other words, the existence of nonclassical intensity correlations is a sufficient condition for entanglement.

The normalized index of intensity correlation between a pair of modes $a_{j,\mathbf{q}}$ and $a_{j',\mathbf{q}'}$ is defined as

$$\gamma_{j,j'}(\mathbf{q},\mathbf{q}') = \frac{\Gamma_{j,j'}(\mathbf{q},\mathbf{q}')}{\sqrt{\langle(\Delta n_{T,\mathbf{q}})^2\rangle\langle(\Delta n_{R,-q})^2\rangle}}, \tag{25}$$

where the correlation term is given by

$$\Gamma_{j,j'}(\mathbf{q},\mathbf{q}') = \langle \Delta n_{j,\mathbf{q}} \Delta n_{j',\mathbf{q}'} \rangle. \tag{26}$$

Upon evaluating the first moments as we did in Eq. (12) we have, for the pair of modes $a_{T,\mathbf{q}}$ and $a_{R,-\mathbf{q}}$,

$$\Gamma_{T,R}(\mathbf{q},-\mathbf{q}) = n_{\text{PDC},\mathbf{q}}(1 + n_{\text{PDC},\mathbf{q}})(1 + \mu_{T,\mathbf{q}} + \mu_{R,-\mathbf{q}})^2 = \mathcal{C}_{\mathbf{q}}^2. \tag{27}$$

A nonzero value of $\Gamma_{T,R}$, and hence of $\gamma_{T,R}$, indicates the presence of correlations between the considered modes. Perfect correlations correspond to $\gamma_{T,R}=1$. Note that $\gamma_{T,R}$ is an increasing function of n_{PDC} and does not undergo any threshold. In Fig. 2 we plot $\gamma_{T,R}$ (solid lines) as a function of n_{PDC} in two different conditions, namely, $\mu_T = 0$ and $\mu_R \neq 0$ [panel (a)] and $\mu_T = \mu_R \neq 0$ [panel (b)]. As expected, $\gamma_{T,R}$ approaches unity irrespective of the mean values of the seeding

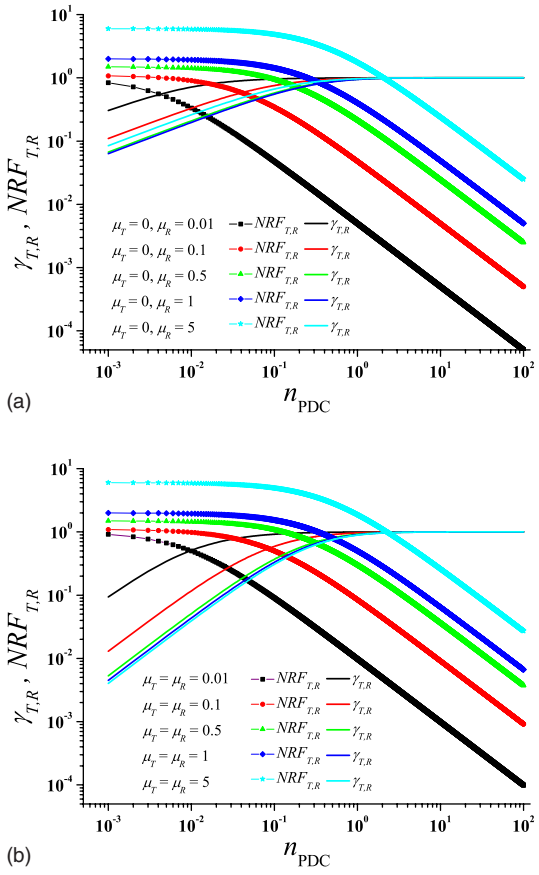

FIG. 2. (Color online) Index of total correlations $\gamma_{T,R}$ (solid lines; legend correlates to lines from top to bottom in figure) and noise reduction factor $\mathrm{NRF}_{T,R}$ (line plus symbol) as a function of n_{PDC} in the cases (a) $\mu_T=0$ and $\mu_R\neq 0$ and (b) $\mu_T=\mu_R\neq 0$. The values chosen for the parameters are indicated in the figures.

thermal fields as soon as n_{PDC} becomes relevant.

For large $n_{\mathrm{PDC},\mathbf{q}}$ the index of correlation approaches unity as follows:

$$\gamma_{T,R}(\mathbf{q},-\mathbf{q}) \simeq 1 - \frac{1}{2}\frac{\mu_{T,\mathbf{q}} + \mu_{R,-\mathbf{q}} + 2\mu_{T,\mathbf{q}}\mu_{R,-\mathbf{q}}}{(1+\mu_{T,\mathbf{q}}+\mu_{R,-\mathbf{q}})^2}\frac{1}{n^2_{\mathrm{PDC},\mathbf{q}}}. \tag{28}$$

In the two cases $\mu_{T,\mathbf{q}}=\mu\gg 1$ and $\mu_{R,-\mathbf{q}}=0$ (or vice versa) and $\mu_{T,\mathbf{q}}=\mu_{R,-\mathbf{q}}=\mu\gg 1$ we have, respectively,

$$\gamma_{T,R}(\mathbf{q},-\mathbf{q}) \simeq 1 - \frac{1}{(1+n_{\mathrm{PDC},\mathbf{q}})n_{\mathrm{PDC},\mathbf{q}}}\frac{1}{2\mu},$$

$$\gamma_{T,R}(\mathbf{q},-\mathbf{q}) \simeq 1 - \frac{1}{(1+2n_{\mathrm{PDC},\mathbf{q}})^2} + O\left(\frac{1}{\mu^2}\right). \tag{29}$$

The nonclassical nature of this pairwise correlation may be assessed by the quantity [14]

$$\mathrm{NRF}_{T,R}(\mathbf{q}) = \frac{\langle(\Delta n_{T,\mathbf{q}})^2\rangle + \langle(\Delta n_{R,-\mathbf{q}})^2\rangle - 2\Gamma_{T,R}(\mathbf{q},-\mathbf{q})}{\langle n_{T,\mathbf{q}}\rangle + \langle n_{R,-\mathbf{q}}\rangle}, \tag{30}$$

which is usually referred to as "the noise reduction factor." A noise reduction, $\mathrm{NRF}_{T,R}(\mathbf{q})<1$, indicates the presence of nonclassical correlations. The value $\mathrm{NRF}_{T,R}(\mathbf{q})=1$ is usually called "shot-noise limit" and corresponds to the case of a pair of uncorrelated coherent signals. By substituting the result for our system, we get

$$\mathrm{NRF}_{T,R}(\mathbf{q}) = \frac{\mu_{T,\mathbf{q}}(1+\mu_{T,\mathbf{q}}) + \mu_{R,-\mathbf{q}}(1+\mu_{R,-\mathbf{q}})}{\mu_{T,\mathbf{q}} + \mu_{R,-\mathbf{q}} + 2n_{\mathrm{PDC},\mathbf{q}}(1+\mu_{T,\mathbf{q}}+\mu_{R,-\mathbf{q}})}. \tag{31}$$

We have $\mathrm{NRF}_{T,R}(\mathbf{q})<1$ if

$$n_{\mathrm{PDC},\mathbf{q}} > \frac{1}{2}\frac{\mu^2_{T,\mathbf{q}} + \mu^2_{R,-\mathbf{q}}}{1+\mu_{T,\mathbf{q}}+\mu_{R,-\mathbf{q}}}, \tag{32}$$

which subsumes the separability threshold of Eq. (23) and individuates the same region for $\mu_{T,\mathbf{q}}=\mu_{R,-\mathbf{q}}$. Therefore, for thermally seeded PDC, sub-shot-noise correlations imply entanglement [15]. In Fig. 2 we also plot $\mathrm{NRF}_{T,R}$ as a function of n_{PDC} for the same parameters used for $\gamma_{T,R}$. As expected, the figure shows that $\mathrm{NRF}_{T,R}$ crosses the shot-noise level at different values of n_{PDC} that depend on the mean values of the thermal seeds, thus confirming the intuition that, in order to achieve sub-shot-noise correlations in the presence of two thermal seeds, we need to have a PDC process strong enough.

IV. MMT-PDC BASED GHOST IMAGING AND GHOST DIFFRACTION

The bipartite state obtained by the nonlinear process described above is suitable for applications to ghost-imaging–ghost-diffraction protocols. Ghost-imaging and ghost-diffraction protocols rely on the capability of retrieving an object transmittance pattern and its Fourier transform, respectively, by the evaluation of a fourth-order correlation function at the detection planes of a light field that has never interacted with the object and a correlated one transmitted by the object. We consider the schemes depicted in Fig. 3. An object, described by the transmission function $t(\mathbf{x}''_T)$, is inserted in the T arm on the plane $\mathbf{x}''_T$ and a bucket detector measures the total light, transmitted by the transparency. The R arm contains an optical setup suitable for reconstructing either the image of the object or its Fourier transform and a position-sensitive detector that measures the local intensity map. The procedure for calculating the correlation function between the light detected in the two arms of the setup is equivalent to evaluating first the correlation function between the intensity operators, which in the Heisenberg picture corresponds to

$$\begin{aligned} G^{(2)}(\mathbf{x}_R,\mathbf{x}_T) &= \mathrm{Tr}[\Delta I_R(\mathbf{x}_R)\Delta I_T(\mathbf{x}_T)\rho_{\mathrm{in}}] \\ &= \mathrm{Tr}[I_R(\mathbf{x}_R)I_T(\mathbf{x}_T)\rho_{\mathrm{in}}] \\ &\quad - \mathrm{Tr}[I_R(\mathbf{x}_R)\rho_{\mathrm{in}}]\mathrm{Tr}[I_T(\mathbf{x}_T)\rho_{\mathrm{in}}], \end{aligned} \tag{33}$$

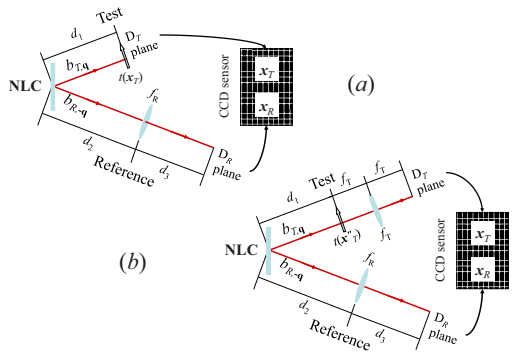

FIG. 3. (Color online) Setup for ghost-imaging and ghost-diffraction experiments: t, object transmission function; $f_{T,R}$, focal length of lenses. (a) Experimental configuration with detection plane coinciding with the object plane, $\mathbf{x}_T=\mathbf{x}_T''$. (b) Experimental configuration with detection plane coinciding with the Fourier plane of the collecting lens in the test arm.

and then integrating over all the values of $\mathbf{x}_T$

$$\mathcal{G}^{(2)}(\mathbf{x}_R)=\int d\mathbf{x}_T G^{(2)}(\mathbf{x}_R,\mathbf{x}_T). \tag{34}$$

In Eq. (33) we have defined the intensity operators as $I_j(\mathbf{x}_j)=c_j^\dagger(\mathbf{x}_j)c_j(\mathbf{x}_j)$ $(j=R,T)$, with $c_j(\mathbf{x}_j)$ the field operators at the detection planes. Thus the average operation in Eq. (33) is taken on the initial state ρ_{in} [see Eq. (5)]. Note that $\text{Tr}[I_j(\mathbf{x}_j)\rho_{\text{in}}]$ are proportional to the detected intensities and that $\text{Tr}[I_R(\mathbf{x}_R)I_T(\mathbf{x}_T)\rho_{\text{in}}]$ is the second-order correlation function [11].

In order to calculate the mean values in Eq. (33), we exploit the connection between the field operators at the detection planes and those at the output of the crystal

$$c_j(\mathbf{x}_i)=\int d\mathbf{x}_j' h_j(\mathbf{x}_j,\mathbf{x}_j')b_j(\mathbf{x}_j'), \tag{35}$$

where $b_j(\mathbf{x}_j')$ are the reference and test field operators at the output face of the crystal [see Eq. (11)] and $h_R(\mathbf{x}_R,\mathbf{x}_R')$ and $h_T(\mathbf{x}_T,\mathbf{x}_T')$ are the two response functions describing the propagation of the field in the two arms of the setup [16].

By using Eqs. (35) and (33) we can rewrite $G^{(2)}(\mathbf{x}_R,\mathbf{x}_T)$ as

$$\begin{aligned}G^{(2)}(\mathbf{x}_R,\mathbf{x}_T)=\int & d\mathbf{x}_R' d\mathbf{x}_R'' d\mathbf{x}_T' d\mathbf{x}_T'' h_R(\mathbf{x}_R,\mathbf{x}_R')h_R^*(\mathbf{x}_R,\mathbf{x}_R'')\\ &\times h_T(\mathbf{x}_T,\mathbf{x}_T')h_T^*(\mathbf{x}_T,\mathbf{x}_T'')\\ &\times\{\text{Tr}[b_R^\dagger(\mathbf{x}_R'')b_R(\mathbf{x}_R')b_T^\dagger(\mathbf{x}_T'')b_T(\mathbf{x}_T')\rho_{\text{in}}]\\ &-\text{Tr}[b_R^\dagger(\mathbf{x}_R'')b_R(\mathbf{x}_R')\rho_{\text{in}}]\text{Tr}[b_T^\dagger(\mathbf{x}_T'')b_T(\mathbf{x}_T')\rho_{\text{in}}]\}.\end{aligned} \tag{36}$$

Equation (36) can be simplified by calculating the factorization rule for $\text{Tr}[b_R^\dagger(\mathbf{x}_R'')b_R(\mathbf{x}_R')b_T^\dagger(\mathbf{x}_T'')b_T(\mathbf{x}_T')\rho_{\text{in}}]$, that is by rewriting the four-points correlation function in terms of the two-points correlation functions [17]. To do this we rewrite $b_j(\mathbf{x})$ in terms of plane waves as $b_j(\mathbf{x})=\mathcal{N}\Sigma_{\mathbf{q}}e^{i\mathbf{q}\cdot\mathbf{x}}b_{j,\mathbf{q}}$ ($\mathcal{N}$ is the normalization coefficient) and then substitute the input-output relations of Eq. (11). After some algebra we obtain

$$\begin{aligned}&\text{Tr}[b_R^\dagger(\mathbf{x}_R'')b_R(\mathbf{x}_R')b_T^\dagger(\mathbf{x}_T'')b_T(\mathbf{x}_T')\rho_{\text{in}}]\\ &=\mathcal{N}^4\sum_{\mathbf{q},\mathbf{q}',\mathbf{q}'',\mathbf{q}'''}e^{-i(\mathbf{q}\cdot\mathbf{x}_R''-\mathbf{q}'\cdot\mathbf{x}_R'+\mathbf{q}''\cdot\mathbf{x}_T''-\mathbf{q}'''\cdot\mathbf{x}_T')}\\ &\times\text{Tr}[b_{R,\mathbf{q}}^\dagger b_{R,\mathbf{q}'}b_{T,\mathbf{q}''}^\dagger b_{T,\mathbf{q}'''}\rho_{\text{in}}]\\ &=\mathcal{N}^4\sum_{\mathbf{q},\mathbf{q}'}e^{-i[\mathbf{q}\cdot(\mathbf{x}_R''-\mathbf{x}_R')+\mathbf{q}'\cdot(\mathbf{x}_T''-\mathbf{x}_T')]}[\mathcal{U}_{\mathbf{q}}^2\mu_{T,\mathbf{q}}\\ &+\mathcal{V}_{\mathbf{q}}^2(1+\mu_{R,-\mathbf{q}})][\mathcal{U}_{\mathbf{q}'}^2\mu_{R,\mathbf{q}'}+\mathcal{V}_{\mathbf{q}'}^2(1+\mu_{T,-\mathbf{q}'})]\\ &+\mathcal{N}^4\sum_{\mathbf{q},\mathbf{q}'}e^{-i[\mathbf{q}\cdot(\mathbf{x}_R''-\mathbf{x}_T'')-\mathbf{q}'\cdot(\mathbf{x}_R'-\mathbf{x}_T')]}[\mathcal{U}_{\mathbf{q}}\mathcal{V}_{-\mathbf{q}}\mu_{T,\mathbf{q}}\\ &+\mathcal{V}_{\mathbf{q}}\mathcal{U}_{-\mathbf{q}}(1+\mu_{R,-\mathbf{q}})][\mathcal{U}_{\mathbf{q}'}\mathcal{V}_{-\mathbf{q}'}(1+\mu_{T,\mathbf{q}'})\\ &+\mathcal{V}_{\mathbf{q}'}\mathcal{U}_{-\mathbf{q}'}\mu_{R,-\mathbf{q}'}].\end{aligned} \tag{37}$$

Performing the same calculation for

$$\begin{aligned}&\text{Tr}[b_R^\dagger(\mathbf{x}_R'')b_R(\mathbf{x}_R')\rho_{\text{in}}]\text{Tr}[b_T^\dagger(\mathbf{x}_T'')b_T(\mathbf{x}_T')\rho_{\text{in}}]\\ &+\text{Tr}[b_R^\dagger(\mathbf{x}_R'')b_T^\dagger(\mathbf{x}_T'')\rho_{\text{in}}]\text{Tr}[b_R(\mathbf{x}_R')b_T(\mathbf{x}_T')\rho_{\text{in}}],\end{aligned} \tag{38}$$

we obtain the same result obtained in Eq. (37). Thus we obtained the noteworthy factorization rule

$$\begin{aligned}&\text{Tr}[b_R^\dagger(\mathbf{x}_R'')b_R(\mathbf{x}_R')b_T^\dagger(\mathbf{x}_T'')b_T(\mathbf{x}_T')\rho_{\text{in}}]\\ &-\text{Tr}[b_R^\dagger(\mathbf{x}_R'')b_R(\mathbf{x}_R')\rho_{\text{in}}]\text{Tr}[b_T^\dagger(\mathbf{x}_T'')b_T(\mathbf{x}_T')\rho_{\text{in}}]\\ &=\text{Tr}[b_R^\dagger(\mathbf{x}_R'')b_T^\dagger(\mathbf{x}_T'')\rho_{\text{in}}]\text{Tr}[b_R(\mathbf{x}_R')b_T(\mathbf{x}_T')\rho_{\text{in}}].\end{aligned} \tag{39}$$

Note that the factorization rule in Eq. (39) obtained for MMT-PDC state is exactly the same obtained for spontaneous PDC [17] and multithermal one-arm-seeded PDC [10]. According to Eq. (39), and in complete analogy with the case of spontaneous PDC [17], also in the case of the MMT-seeded PDC we obtain

$$\begin{aligned}G^{(2)}(\mathbf{x}_R,\mathbf{x}_T)=\Bigg|\int d\mathbf{x}_R'\int d\mathbf{x}_T' h_R(\mathbf{x}_R,\mathbf{x}_R')h_T(\mathbf{x}_T,\mathbf{x}_T')\\ \times\text{Tr}[b_R(\mathbf{x}_R')b_T(\mathbf{x}_T')\rho_{\text{in}}]\Bigg|^2,\end{aligned} \tag{40}$$

where

$$\begin{aligned}&\text{Tr}[b_R(\mathbf{x}_R')b_T(\mathbf{x}_T')\rho_{\text{in}}]\\ &=\mathcal{N}^2\sum_{\mathbf{q},\mathbf{q}'}e^{i(\mathbf{q}\cdot\mathbf{x}_R'+\mathbf{q}'\cdot\mathbf{x}_T')}\text{Tr}[b_{R,\mathbf{q}}b_{T,\mathbf{q}'}\rho_{\text{in}}]\\ &\propto\sum_{\mathbf{q},\mathbf{q}'}e^{i[\mathbf{q}\cdot(\mathbf{x}_T'-\mathbf{x}_R')+\varphi_{\mathbf{q}}]}(\mathcal{U}_{\mathbf{q}}\mathcal{V}_{\mathbf{q}'}\text{Tr}[a_{R,\mathbf{q}}a_{R,-\mathbf{q}'}^\dagger\rho_{\text{in}}]\\ &+\mathcal{V}_{\mathbf{q}}\mathcal{U}_{\mathbf{q}'}\text{Tr}[a_{T,-\mathbf{q}}^\dagger a_{T,\mathbf{q}'}\rho_{\text{in}}])\\ &=\sum_{\mathbf{q}}e^{i[\mathbf{q}\cdot(\mathbf{x}_T'-\mathbf{x}_R')+\varphi_{\mathbf{q}}]}\mathcal{C}_{\mathbf{q}}.\end{aligned} \tag{41}$$

By using Eq. (41), Eq. (40) can be rewritten as

$$G^{(2)}(\mathbf{x}_R,\mathbf{x}_T)\propto\left|\sum_{\mathbf{q}}\tilde{h}_R(\mathbf{x}_R,-\mathbf{q})\tilde{h}_T(\mathbf{x}_T,\mathbf{q})\mathcal{C}_{\mathbf{q}}\right|^2, \tag{42}$$

where $\tilde{h}_j(\mathbf{x}_j,\mathbf{q})=\int d\mathbf{x}_j' e^{i\mathbf{q}\cdot\mathbf{x}_j'}h_j(\mathbf{x}_j,\mathbf{x}_j')$.

According to Fig. 3, we consider the following two different schemes for the collection optics in the test arm of the setup.

(a) The detection plane coincides with the plane of the transparency, $\mathbf{x}_T=\mathbf{x}_T''$, and hence

$$\tilde{h}_T(\mathbf{x}_T,\mathbf{q}) \propto e^{-i(\lambda d_1/4\pi)q^2} e^{-i\mathbf{q}\cdot\mathbf{x}_T} t(\mathbf{x}_T) \tag{43}$$

only describes free propagation over a distance d_1.

(b) A collection lens f_T is located beyond the transparency at a distance f_T from the detection plane, so that the detection plane coincides with that of the Fourier transform, and hence

$$\tilde{h}_T(\mathbf{x}_T,\mathbf{q}) \propto e^{-i(\lambda d_1/4\pi)q^2} \tilde{t}\left(-\mathbf{q}-\frac{2\pi}{\lambda f_T}\mathbf{x}_T\right). \tag{44}$$

The optical scheme in the reference arm contains a lens (focal length f_R) located at $\mathbf{x}_{l,R}$ and thus the Fourier transform of the impulse response functions can be written as

$$\begin{aligned}\tilde{h}_R(\mathbf{x}_R,-\mathbf{q}) &\propto \int d\mathbf{x}_R' e^{-i\mathbf{q}\cdot\mathbf{x}_R'} \int d\mathbf{x}_{l,R} e^{i(\pi/\lambda d_2)(\mathbf{x}_{l,R}-\mathbf{x}_R')^2} e^{-i(\pi/\lambda f_R)\mathbf{x}_{l,R}^2} e^{i(\pi/\lambda d_3)(\mathbf{x}_{l,R}-\mathbf{x}_R)^2} \\ &\propto e^{-i(\lambda d_2/4\pi)q^2} \int d\mathbf{x}_{l,R} e^{-i[(2\pi/\lambda d_3)\mathbf{x}_R+\mathbf{q}]\cdot\mathbf{x}_{l,R}} e^{i(\pi/\lambda)(1/d_3-1/f_R)\mathbf{x}_{l,R}^2}.\end{aligned} \tag{45}$$

If $f_R \neq d_3$, Eq. (45) becomes

$$\tilde{h}_R(\mathbf{x}_R,-\mathbf{q}) \propto e^{-i(\lambda/4\pi)[d_2+1/(1/d_3-1/f_R)]q^2} e^{-(i/d_3)[1/(1/d_3-1/f_R)]\mathbf{q}\cdot\mathbf{x}_R}, \tag{46}$$

while if $f_R=d_3$, Eq. (45) becomes

$$\tilde{h}_R(\mathbf{x}_R,-\mathbf{q}) \propto e^{-i(\lambda d_2/4\pi)q^2} \delta\left(\frac{2\pi}{\lambda d_3}\mathbf{x}_R+\mathbf{q}\right). \tag{47}$$

Depending on the chosen geometrical configuration, these schemes allow realization of either a ghost-imaging or a ghost-diffraction experiment [18], as explained below.

A. Ghost imaging

To perform a ghost-imaging experiment we choose $f_R \neq d_3$.

Let us first consider case (a). Substituting Eq. (43) and Eq. (46) into Eq. (42) yields the expression

$$G^{(2)}(\mathbf{x}_R,\mathbf{x}_T) \propto |t(\mathbf{x}_T)|^2 \left| \sum_{\mathbf{q}} \mathcal{C}_{\mathbf{q}} e^{-i\mathbf{q}\cdot\{\mathbf{x}_T+(1/d_3)[1/(1/d_3-1/f_R)]\mathbf{x}_R\}} e^{-i(\lambda/2\pi)[(d_1+d_2)/(1/d_3-1/f_R)][1/(d_1+d_2)+1/d_3-1/f_R]q^2} \right|^2 \simeq |t(\mathbf{x}_T)|^2 |\mathcal{C}_{\mathbf{q}}|^2 \delta\left(\mathbf{x}_T+\frac{\mathbf{x}_R}{M}\right), \tag{48}$$

which, once integrated over the bucket detector,

$$\mathcal{G}^{(2)}(\mathbf{x}_R) = \int d\mathbf{x}_T G^{(2)}(\mathbf{x}_R,\mathbf{x}_T) \simeq \left| t\left(-\frac{\mathbf{x}_R}{M}\right) \right|^2 |\mathcal{C}_{\mathbf{q}}|^2, \tag{49}$$

gives the image of the object. Note that in passing from Eq. (48) to Eq. (49) we have assumed that $\mathcal{C}_{\mathbf{q}}$ is virtually independent of $\mathbf{q}$. Moreover, we have chosen distances d_1, d_2, and d_3 that satisfy the so-called "back-propagating thin lens equation," $1/(d_1+d_2)+1/d_3=1/f_R$ [19], so that we obtain an imaging system with magnification factor $M=d_3/(d_1+d_2)$.

In case (b), that is with a collection lens in the test arm that forms the Fourier transform on the detection plane, we proceed similarly by substituting Eq. (44) and Eq. (46) into Eq. (42) and making the same assumption or choice as before and obtain

$$G^{(2)}(\mathbf{x}_R,\mathbf{x}_T) \propto \left| \sum_{\mathbf{q}} \mathcal{C}_{\mathbf{q}} \tilde{t}\left(-\mathbf{q}-\frac{2\pi}{\lambda f_T}\mathbf{x}_T\right) e^{-i(1/d_3)[1/(1/d_3-1/f_R)]\mathbf{q}\cdot\mathbf{x}_R} e^{-i(\lambda/2\pi)[(d_1+d_2)/(1/d_3-1/f_R)][1/(d_1+d_2)+1/d_3-1/f_R]q^2} \right|^2 \simeq \left| t\left(-\frac{\mathbf{x}_R}{M}\right) \right|^2 |\mathcal{C}_{\mathbf{q}}|^2, \tag{50}$$

which is independent of $\mathbf{x}_T$. Note that in this case to obtain the image of the object it is not necessary to perform the integration over the bucket detector; we only need to pick up a single point in the Fourier plane, that is we select a single Fourier component.

B. Ghost diffraction

To perform a ghost-diffraction experiment we consider the configuration $d_3=f_R$ and choose configuration (b) in the test arm. By inserting Eq. (44) and Eq. (47) into Eq. (42)

$$G^{(2)}(\mathbf{x}_R,\mathbf{x}_T) \propto \left| \sum_{\mathbf{q}} \mathcal{C}_{\mathbf{q}} \tilde{t}\left(-\mathbf{q}-\frac{2\pi}{\lambda f_T}\mathbf{x}_T\right) e^{-i(\lambda/4\pi)(d_1+d_2)q^2} \times \delta\left(\frac{2\pi}{\lambda d_3}\mathbf{x}_R-\mathbf{q}\right)\right|^2 \simeq \left|\tilde{t}\left(-\frac{2\pi}{\lambda d_3}\mathbf{x}_R-\frac{2\pi}{\lambda f_T}\mathbf{x}_T\right)\right|^2 |\mathcal{C}_{\mathbf{q}}|^2. \quad (51)$$

By selecting the Fourier component detected at $\mathbf{x}_T=0$ we get

$$G^{(2)}(\mathbf{x}_R,0) \simeq \left|\tilde{t}\left(-\frac{2\pi}{\lambda d_3}\mathbf{x}_R\right)\right|^2 |\mathcal{C}_{\mathbf{q}}|^2, \quad (52)$$

which gives the diffraction pattern of the object. Note that the choice of a point different from $\mathbf{x}_T=0$, that is of a different Fourier component, would imply a translation of the recovered diffraction pattern. For this reason a bucket detector, which would perform an integration over the spatial Fourier components, cannot be used. For the same reason also choosing scheme (a) would not give any result, as in this scheme each point $\mathbf{x}_T$ collects light from different spectral components.

V. CONCLUSIONS AND OUTLOOKS

This paper was aimed at showing the possibility of performing ghost imaging and ghost diffraction with a source based on PDC seeded with MMT fields in both the T and R arms, which generates a bipartite correlated state. Peculiar properties of this source may open an insight into the understanding of the ghost-imaging–ghost-diffraction process. In fact, nowadays the sources considered for ghost imaging and diffraction were either definitely separable (classically correlated beams obtained from a MMT source) or entangled (spontaneous PDC). On the contrary, here we proved that the separable or entangled nature of the light produced by our source can be controlled by changing the seed intensities and that the transition from quantum to classical regimes does not modify the possibility of realizing ghost-imaging schemes.

Furthermore, we also showed that a ghost-imaging experiment performed with our source satisfies the "back-propagating" thin-lens equation, as much as with spontaneous PDC, even when the state produced becomes separable. This is in contrast with the idea, also recently suggested [7–9], that the "back-propagating" thin-lens equation is connected with the entangled nature of the spontaneous PDC.

According to the consideration above, we are planning to realize a ghost-imaging experiment with a MMT seeded PDC source in order to show that the same optical configuration allows retrieval of the image irrespective of the entangled or separable nature of the light produced by the source. This will definitely substantiate our claim that the "back-propagating" thin-lens equation is not a signature of entanglement.

ACKNOWLEDGMENTS

This work has been supported by MIUR Projects No. PRIN2005024254-002 and No. FIRB-RBAU014CLC-002.

[1] T. B. Pittman, Y. H. Shih, D. V. Strekalov, and A. V. Sergienko, Phys. Rev. A **52**, R3429 (1995).
[2] D. V. Strekalov, A. V. Sergienko, D. N. Klyshko, and Y. H. Shih, Phys. Rev. Lett. **74**, 3600 (1995); P. H. S. Ribeiro, S. Padua, J. C. MachadodaSilva, and G. A. Barbosa, Phys. Rev. A **49**, 4176 (1994).
[3] M. D'Angelo and Y. H. Shih, Laser Phys. Lett. **2**, 567 (2005); A. Gatti, M. Bache, D. Magatti, E. Brambilla, F. Ferri, and L. A. Lugiato, J. Mod. Opt. **53**, 736 (2006); Y. Shih, e-print arXiv:0707.0268; A. Gatti, M. Bondani, L. A. Lugiato, M. G. A. Paris, and C. Fabre, Phys. Rev. Lett. **98**, 039301 (2007).
[4] A. Valencia, G. Scarcelli, M. D'Angelo, and Y. Shih, Phys. Rev. Lett. **94**, 063601 (2005).
[5] D. Zhang, Y. H. Zhai, L. A. Wu, and X. H. Chen, Opt. Lett. **30**, 2354 (2005).
[6] F. Ferri, D. Magatti, A. Gatti, M. Bache, E. Brambilla, and L. A. Lugiato, Phys. Rev. Lett. **94**, 183602 (2005).
[7] D.-Z. Cao, J. Xiong, and K. Wang, Phys. Rev. A **71**, 013801 (2005).
[8] Y. Cai and S. Y. Zhu, Opt. Lett. **29**, 2716 (2004).
[9] Y. Cai and S. Y. Zhu, Phys. Rev. E **71**, 056607 (2005).
[10] E. Puddu, A. Andreoni, I. P. Degiovanni, M. Bondani, and S. Castelletto, Opt. Lett. **32**, 1132 (2007); for the generalization to multiple parametric processes see, e.g., A. Ferraro, M. G. A. Paris, M. Bondani, A. Allevi, E. Puddu, and A. Andreoni, J. Opt. Soc. Am. B **21**, 1241 (2004); M. Bondani, A. Allevi, E. Puddu, A. Andreoni, A. Ferraro, and M. G. A. Paris, Opt. Lett. **29**, 180 (2004).
[11] L. Mandel and E. Wolf, *Optical Coherence and Quantum Optics* (Cambridge University Press, Cambridge, UK, 1995).
[12] D. R. Truax, Phys. Rev. D **31**, 1988 (1985).
[13] R. Simon, Phys. Rev. Lett. **84**, 2726 (2000).
[14] A. Agliati, M. Bondani, A. Andreoni, G. De Cillis, and M. G. A. Paris, J. Opt. B: Quantum Semiclassical Opt. **7**, S652 (2005).
[15] M. Bondani, A. Allevi, G. Zambra, M. G. A. Paris, and A. Andreoni, Phys. Rev. A **76**, 013833 (2007).
[16] J. W. Goodman, *Fourier Optics* (McGraw-Hill, New York,

1968).

[17] E. Brambilla, A. Gatti, M. Bache, and L. A. Lugiato, Phys. Rev. A **69**, 023802 (2004); A. Gatti, E. Brambilla, M. Bache, and L. A. Lugiato, Phys. Rev. Lett. **93**, 093602 (2004); A. Gatti, E. Brambilla, M. Bache, and L. A. Lugiato, Phys. Rev. A **70**, 013802 (2004).

[18] A. Gatti, E. Brambilla, and L. A. Lugiato, Phys. Rev. Lett. **90**, 133603 (2003); J. C. Howell, R. S. Bennink, S. J. Bentley, and R. W. Boyd, *ibid.* **92**, 210403 (2004); M. D'Angelo, Y. H. Kim, S. P. Kulik, and Y. Shih, *ibid.* **92**, 233601 (2004).

[19] A. F. Abouraddy, B. E. A. Saleh, A. V. Sergienko, and M. C. Teich, J. Opt. Soc. Am. B **19**, 1177 (2002).